Mathematically Modeling Chondrocyte Orientation and division in Relation to Primary Cilium

Christian Blanco, Ian Drayer, Hannah Kim, Ryan Wilson

August 6, 2010

1 Introduction

Confocal microscopy images show that growth plate chondrocytes will tend to form columns after cellular division[2], and the primary cilium may be responsible for the migration of the cells[4][5]. These cells have the ability to move within the growth plate, possibly influenced by the environment, and the primary cilium may direct the orientation and positioning of the cell in response to the environment or extracellular matrix[13][10][15][19][8][22][24]. The primary cilium may also point in the direction of movement of cells or cell formation[20], and that cell movement may be related to hardness or softness of the surface[23]. It has been demonstrated that cells divide perpendicular to the growth plate before moving into columns[6].

The cells may react differently to stimuli based upon their level of development[12], and the development of the cells can be influenced by a mutation. In particular, the disruption of IFT can cause chondrocytes to no longer form in a columnar structure[21] and knockouts of Smad 1, 5, and 8 cause increased apoptosis[18]. The primary cilium has been shown to be related to the centrioles, and that the centrioles are related to cell division and positioning[1][7].

Previous mathematical models are broken into three categories; ones that look at longitudinal bone length as a differential equation with respect to time, ones that view the bone as broken into various regions and models the growth of each of them, and ones that model individual cellular division without concern to the large-scale full bone growth. Classic examples include modeling the length of gull wings as they age [11], as well as fluid and mass flow through the zones of the growth plate using coupled partial differential equations [9]. Individual cell division was modeled using ovals of Cassini to represent one mother cell dividing into two daughter cells [14].

The value of the ϕ_{ci} for the wild type clusters at around both 10 degrees and 80 degrees, as opposed to the value of the ϕ_{ci} of the mutant whose ϕ_{ci} clusters only at approximately 80 degrees. Because the growth plate of the wild type mouse is more organized than the mutant mouse, we utilized the idea that the ϕ_{ci} clustering at around 10 degrees, which does not occur in the mutant, controls the organization of the growth plate of the wild type mouse. Therefore, we made the assumption that the closer the value of ϕ_{ci} is to 0 degrees, the stronger the signal emitted.

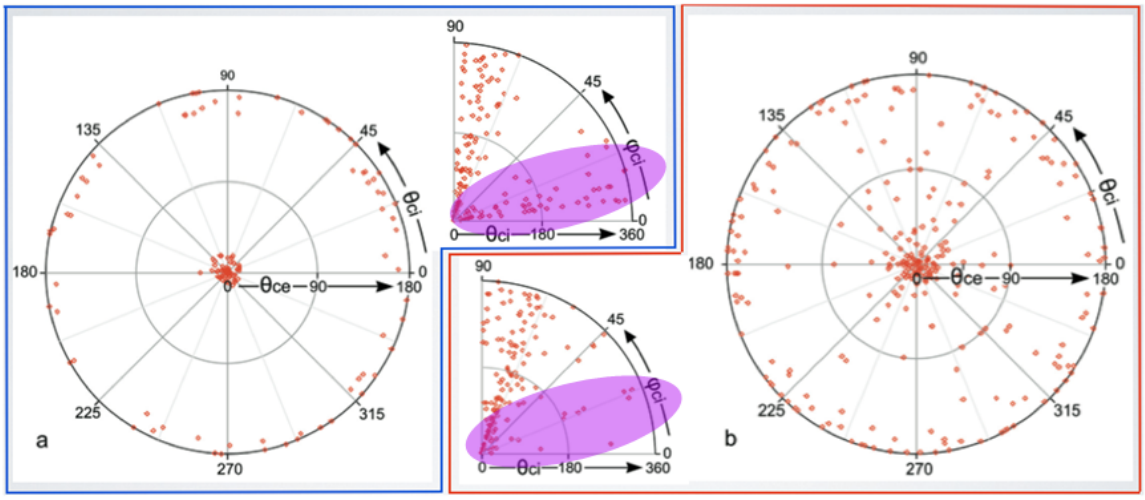

Figure 1: A comparison of $\theta_{ce}, \theta_{ci}, \phi_{ci}$ data for Wild Type and SMad1/5^{CKO}. The WT appears on the left enclosed in the blue box while the mutant appears on the right in the red box. Note the absence of cells with $\phi_{ci} = 10$ in the mutant.

2 Models

These models are based on the idea that the chondrocytes in the growth plate interact with one another during cell division through a signaling mechanism based on the orientation of the primary cilium. The signal may be global (affects all nearby cells) or local (affects only daughter cell) within the proliferative zone. We considered the signaling intensity to be a scalar quantity subject to the superposition principle. The dependency on intensity was chosen so that the distribution of modeled ciliary angle ϕ of the wild type mouse follows the distribution of the experimental data.

Our first, basic model randomly placed ellipses to model cells on the xy-plane of the growth plate. Each ellipse was defined in terms of major and minor axes and theta, the angle of major axis with respect to the horizontal (x) axis chosen from the experimental distributions of mutant and wild type. The only restriction was that if the daughter cell overlapped one of the existing cells, it would not be drawn. This process was repeated for a specified number of cells.

2.1 Cellular Interaction

Our interaction model is based on the distribution of ϕ_{ci}. We chose to use a cosine function to model the decreasing signal as the angle approaches 90 degrees because it has a maximum at 0 degrees and is 0 at 90 degrees. We then modeled the dispersion of this signal based upon the dispersion of a sound wave in 3 dimensions. We therefore used an inverse squared relationship with distance. We then multiplied by a scaling factor κ in order to determine the intensity at a cell i caused by cell j (eq. 1). For each cell, we then placed these intensity values in a matrix that we termed the "Matrix of Dependencies". The total intensity at any given cell was obtained by adding the rows of the matrix of dependencies (eq. 2). This total intensity is used to determine the steepness of the hyperbolic tangent function that is used to determine the new theta angle of the cells (eq. 3).

$$f_{i,j}(\phi_i, d_{i,j}) = \kappa \frac{\cos(\phi_i)}{d_{i,j}^2} \text{for} i \neq j \tag{1}$$

$$b_j = \sum_{i \neq j} f_{i,j} \tag{2}$$

$$\theta_{ce_{new}}(b, \theta_{ce_{ran}}) = \begin{cases} \theta_{ce_{ran}} \tanh\left(b(\theta_{ce_{ran}} - \frac{\pi}{2})\right) + \theta_{ce_{ran}} & : 0 < x \leq \frac{\pi}{2} \\ (\theta_{ce_{ran}} - \frac{\pi}{2}) \tanh(b(-\theta_{ce_{ran}} + \frac{\pi}{2})) + \theta_{ce_{ran}} & : \frac{\pi}{2} < x \leq \pi \end{cases} \tag{3}$$

We modified the hyperbolic tangent in order to create a distribution that approximates that of the experimental wild type data when there is higher signal, and that is a straight line when there is no signal, indicating a uniform random distribution of cell theta angles. This function is utilized by inputting a random value from the uniform distribution of 0 to π for $\theta_{ce_{ran}}$. The function outputs an angle between 0 and π, with the distribution of angles for θ_{ce} conforming to the distribution of the experimental data. As the intensity, b, increases, the steepness of the function increases, causing a greater number of random θ's to be placed closer to 0 or π.

2.2 Interaction model with forced columnar structure

Our next model took into account the intercellular interactions with a forced columnar structure, where a cell was initially placed with θ_{ce} chosen from the distribution of the experimental data. One cell from the column was randomly selected as the dividing cell. All cells below the chosen dividing cell were moved down by a fixed distance, while a new cell with random specification of size and orientation was inserted at the now empty position. The center of the daughter cell was placed at a fixed distance from the mother cell's center along the minor axis of the mother cell. We then computed new orientations for all the cells based upon our function (eq. 3. This algorithm was repeated to form a column of any number of cells. This model failed to produce any discernable difference between the mutant and wild type due to the forced columnar positioning with constant x values for the cells.

2.3 Columnar interaction model with position variation

Our next model allowed for variation in the x position of the daughter cells. After generating one cell with specifications $(\theta_{ce}, \theta_{ci}, \phi_{ci})$ selected from the distribution, we randomly selected a cell to divide, and generated a new cell with identical θ_{ce}. It was placed at a constant distance from the mother cell along the major axis of the mother cell and moved all cells underneath the new cell down in order to prevent intersection between cells. Once again, eq. 3 was applied to the cells at each stage of division. This method gives the wild type a columnar appearance, while the model of the mutant growth plate acquires a more disorganized pattern, while mutant simulations produced cells varying both left and right in x position. This model produced a large difference in appearance in cell organizations of wild type mutant, and produced statistically significant differences in our "columnness" values. "Columnness" here is a measure of how well of a column is formed. We found that the average columnness of the wild type was statistically significantly $(p < 0.0001, \bar{C_{dev}}_m ut - \bar{C_{dev}}_w t = 0.641$ higher the average columnness of the mutant.

2.4 Multi-column model with columnar interaction

Our final model initializes the same way as the previous model, generating one random cell. Then one cell is selected for division from those already formed its center point is saved. Then generate a new θ_{ce} from a distribution based upon our intensity at that point and rotate the cell that is to divide. The new cell centers are placed outside the mother cell's center at a fixed distance along the minor axis of the mother cell. Because there is no signal for the first cell, the first cell is likely to divide parallel to the growth plate and cause multiple columns to form. We separated the formed cells to prevent overlap, moving the cells downward if they are below the dividing cell, and moving the cells upward if they are above the dividing cell. The multiple columns of cells tend to line up as the intensity increases, with the θ_{ce} values following the distribution of the experimental data.

2.5 Spatial Optimization

We model cell movement using non-linear optimization. Our spatial optimization is given by::

$$\begin{aligned} \underset{x_i, y_i}{\text{minimize}} \quad & \sum_i \sqrt{\alpha cos(\phi)(x_i^{(0)} - x_i)^2 + (y_i^{(0)} - y_i)^2} \\ \text{subject to} \quad & 0 \geq s - \sqrt{(x_i - x_j)^2 + \beta(y_i - y_j)^2}, \text{ for } j > i \\ & 0 \geq -x_i \\ & t \geq x_i \end{aligned} \tag{4}$$

The motivation behind minimizing the change in the cell's original position is to minimize cellular movement, which requires energy. The α term is a penalty factor, which makes it more difficult to move in the x-direction, which gives a preferential movement in the y direction. Similarly, we constrain the distance of the cells, so that cells do not overlap each other. Currently the constraints are written for global cellular interaction (all cells interact with each other). This does not pose a problem for cells that are a distance s away, since their constraints are automatically satisfied. The optimization condition is currently written with radial distance constraints, causing the cells to arrange in diamonds, and not necessarily columns. We decided to add a β factor in the conditions to increase the bias in movement in the y-direction. We want the cells to move in the direction of bonegrowth (y-direction) as opposed to the x-direction. We test for different parameters, and apply the spatial optimization to the mutant spatial distribution to see preliminary results.

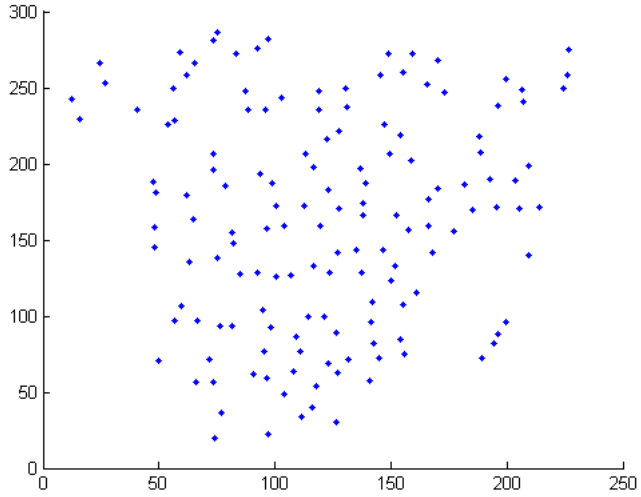

Mutant Spatial Distribution

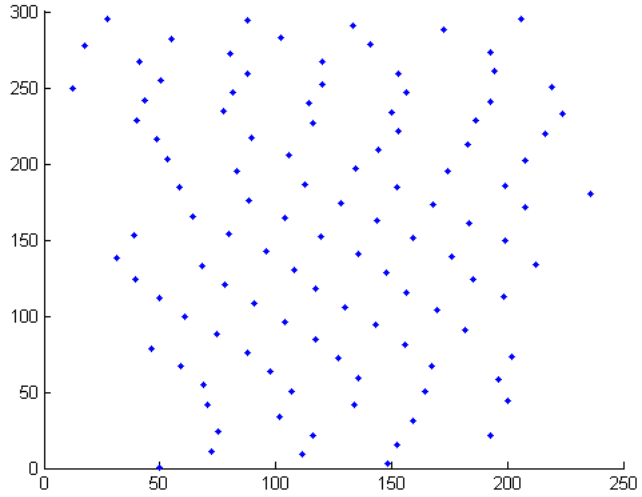

After Spatial Optimization

with parameters:

$$t = 260 \qquad s = 35$$
$$\alpha = 100 \qquad \beta = 10$$
$$\phi = 0$$

We also did scenarios where we only applied the optimization in various $x \in [a, b]$. For example we only optimize all the cells within an interval $x_i \in [0, 20]; x_i \in [20, 40]; ....$

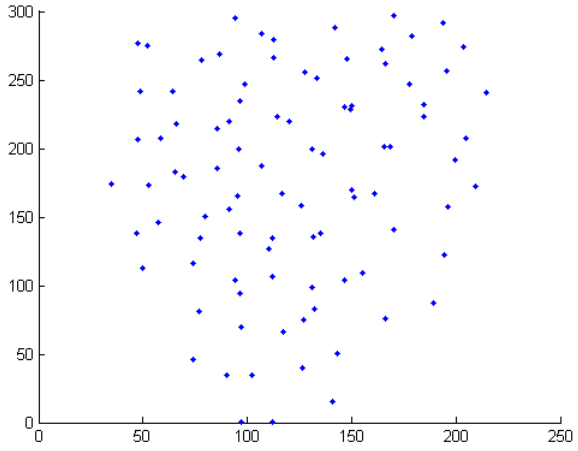

Optimization 1: with parameters $t = 260$
$s = 20$ $\alpha = 100$ $\beta = 1$ $\phi = 0$
intervals of 10

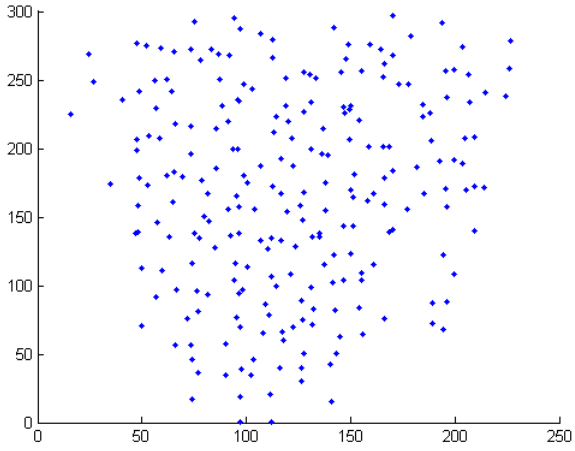

Optimization 2: with parameters $t = 240$
$s = 35$ $\alpha = 20$ $\beta = 1$ $\phi = 0$
intervals of 20

Notice that optimization 1 shows less cells compared to optimization 2. This is due to cells shooting out of the axis of interest. We ran other simulations where parameters caused too much regularity and moved

cells up to 900. We ignored these simulations simply because they seemed unrealistic. These parameters given here, show more reasonable parameters. Further test of changing the ϕ_{ci} value will further confirm the accuracy of the model with respect to the orientation of the primary cilia. The algorithms that we have presented so far provide a blackbox of functions for recreating spatial patterns with the ϕ orientation of the cilia as a crucial input for the functions. This model simply accounts for the cell output signals, and does not explain cell signal input nor does it cover cell-ECM interactions. In addition, these models only provide spatial pattern recreation, and does not necessarily incorporate cell biomechanics. Some of the scenarios produce here were useful in providing dummy simulations to test against the $\hat{C}$-function. A call for a more detailed cell-mechanics modeling is needed. In the next models, we provide further notes and other possible cell-cell and cell-ECM interactions. These biomechanical models may be adopted and improved further to incorporate or explain the difference in the ϕ.

3 Cell-ECM interactions

This section of the paper is a literature review for further investigation in mathematical modeling of cell stress/strain and its interaction with the ECM. We have not implemented any of the following models, but they provide further insight into future approaches in modeling cellular mechanics, and a call for adding the orientation of the primary cilia. It is be possible that the orientation of the primary cilia is experiencing a confounding effect where its orientation is dependent on its environment, and possibly not the other way around where the environment is depend on the primary cilia. Although, it has been hypothesized that the primary cilia acts as a mechanosensor or chemosensor, it could be possible that the orientation of the primary cilia is dependent on stresses and strain of the ECM. Similarly, we also hypothesize that ciliated chondrocytes initially orients the primary cilia in the direction of $\phi = 90$, but due to stresses and strain in the ECM and its environment, the primary cilia bends to $\phi_{ci} = 0$. It could also be possible that the primary cilia in the orientation of $\phi = 0$ activates certain biomechanisms in the cell (compressibility, activation of the cell to perform a certain role, etc.). In the mutant scenario, the orientation of ϕ is bias towards 90 degress. This observation maybe due to the lack of stress and strain in the ECM or the environment of the chondrocyte. We hypothesize that after cellular division, the orientation of the primary cilia is biased to $\phi = 90$ Only in the presence of stresses and strain does the primary cilia reorient itself.

Although there is dominant columnar organization in WT, we also notice minute columnar tendencies. Looking closely at the images, sometimes we also notice radial symmetry. Are chondrocytes bias towards a columnar formation because this orientation allows for perfrorming less work? Does stacking minimize the total work exerted by individual cells in the proliferative zone? If this is the case, what is preventing chondrocytes from forming columns in mutant $Smad1/5^{CKO}$? This gene can be necessary for the cell to orient its ECM correctly or to interact with other cells properly. A call for biological experiments is need to answer the following questions: what type of biomechanical properties are preserved in mutant compared to WT? Without further biological experiments, it may be difficult to mathematically model chondorcyte pattern formation, simply because there could be two or more mechanisms acting together that are also lost with the knockout, and our current model only attributes all mechanisms to one organelle: the primary cilia.

3.1 Mechanical modelling of cell/ECM and cell/cell interactions: theory and model simulation [17]

by: Ramtani

3.1.1 Overview

n	Local cell concentration(density)
ρ	local ECM concentration
$\mathbf{r}$	Position vector for cell-ECM composite
u_i	displacement for cell-ECM composite
T_{ij}	total stress tensor for cell-ECM composite
σ_{ij}	stress tensor for ECM
τ_{ij}	stres tensor associated with the cell-ECM interaction
π_{ij}	stress tensor associated with the cell-cell interactions
ϵ_{ij}	small strain tensor for cell-ECM composite
E	Young's modulus
ν	Poission ratio
μ_1	shear viscosity
μ_2	bulk viscosity
δ_{ij}	identity tensor
τ^0	traction parameter
λ	contact inhibition parameter
v	velocity of cell-ecm composite
α	cell-cell traction force

Let T_{ij} be the total stress tensor for the cell-ECM composite:

$$T_{ij} = \sigma_{ij} + \tau_{ik}u_{j,k} + \pi_{ij} \tag{5}$$

where σ_{ij}, τ_{ik}, and pi_{ij} are the ECM, cell-ECM, and cell/cell interactions.

We further describe the stress-strain for the ECM:

$$\sigma_{ij} = \mu_1 \frac{\partial \epsilon_{ij}}{\partial t} + \mu_2 \frac{\partial \epsilon_{kk}}{\partial t}\delta_{ij} + \frac{E}{(1+\nu)}[\epsilon_{ij} + \frac{\nu}{1-2\nu}\epsilon_{kk}\delta_{ij}] \tag{6}$$

where ϵ_{ij} is the linearized strain tensor, δ_{ij} is the identity tensor, u_1, u_2 are related to the shear and bulk viscosities, and E is the Young's modulus and ν is the Poission ratio.

Cell-ECM interaction force

$$\tau_{ij} = -\frac{\tau^0 \rho}{1+\lambda n^2} n\delta_{ij} \tag{7}$$

The stress τ_{ij} has been considered as a "negative pressure." λ defines the saturation cell density, and τ^0 is a measure of the traction exerted by a cell on local ECM fibers (reflecting the innate ability of the cell to generate motile force and the efficiency with which the cell transmits the force to fibrils via pseudopod-fiber interaction.

Cell-Cell interaction

$$\pi_{ij} = \sum_k \alpha_k(\mathbf{r}) \frac{n_k}{(\mathbf{r}-\mathbf{r_k})^2} n\delta_{ij} \tag{8}$$

where $\alpha_k(\mathbf{r})$ is a measure of the traction exerted by a cell at location $\mathbf{r}_k$ on the cell at location $\mathbf{r}$, at a constant value α. If we neglect inertial forces, the equation of motion is given by:

$$(\sigma_{ij} + \tau_{ik}u_{j,k} + \pi_{ij})_j = 0 \tag{9}$$

3.1.2 Notes and Takeaway

From the literature, one possible scenario of dependencies can be viewed in the following way:

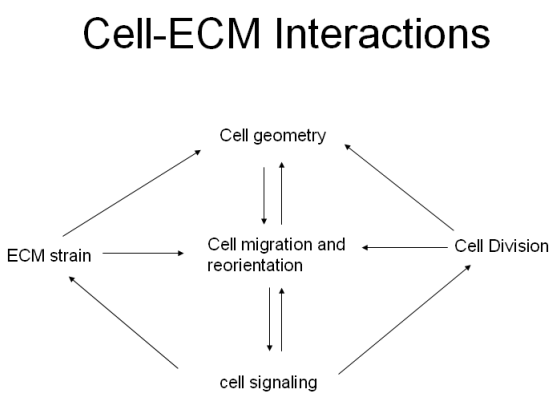

3.2 Cell organization in soft media due to active mechanosensing [3]

By: I.B. Bischofs and U.S Schwarz

3.2.1 Overview

Hypothesis: cells strengthen contacts and cytoskeleton in the direction of large effective stiffness. They model optimal cell organization in the ECM using linear elasticity theory. "Cells orient in the direction of external tensile strain; they orient parallel and normal to free and clamped surfaces."

Cells position and orient themselves such that it senses maximal effective stiffness in its environment. Most important input is the elasticity of the surrounding environment. They model how stress and strain in ECM affect the cell. In this model, they assume that the medium is isotropic. Here we need two elastic moduli: Young modulus E (in kilopascals), and Poission ratio ν. The relationship between the stiffness tensor gives the relationship between stress (internal force) and strain (deformation). For isotropic mediums, there is no preference for direction, but any applied force will give the same displacement depending on the direction of the force. The stiffness tensor is written as:

$$C_{ijkl} = K\delta_{ij}\delta_{kl} + \mu(\delta_{ik}\delta jl + \delta_{il}\delta_{jk} - \frac{2}{3}\delta_{ij}\delta_{kl}) \tag{10}$$

The model tries to predict which way the cell will organize itself according to its environment by actively sensing and pulling on it. The cell has to exert some work W into the surrounding elastic medium to build force F at the contact position $\hat{r_c}$. The cell invests less work W_0 to achieve a certain force F when rigidity E increases. This means that the cell senses maximal stiffness at the contact when W_0 is minimal. In a

homogenous medium, elastic constants don't change and W_0 remains the same. But the work needed to build up force at the contact position r_c changes due to prestrain. The change in W is given by:

$$\Delta W = \int d^3 r C_{ijkl} u^c_{ij}(r) u^c_{kl}(r) = F \cdot u_e(r_c) \tag{11}$$

Where $u^c_{ij}(r)$ is the corresponding strain tensor, and u_e is the displacement caused by the external strain. A negative ΔW represents an effective stiffening of the environment, and a positive ΔW represents a softening with respect to unstrained medium. W quantifies the local elastic input available to an actively mechanosensing cell within the unifying concept of effective stiffness, regardless of its original physical state. The optimal cell position and orientation with the specific force pattern that minimizes the quantity W. This orientation corresponds to a cellular preference for maximal effective stiffness in the local environment. According to the model, the cell is not assumed to minimize W, but instead for different parameters, W measures the kind of information a cell can extract from its elastic environment through mechanosensing. On the otherhand, the model can also be used to describe a mechanism for cellular preference for effective stiffness, in which case uses the quantity W to characterize the cell's internal mechanism.

The model characterizes the mechanical properties of the ECM sensed by the cell, and not the way cells sense its environment. Suppose the ECM acts as a linear spring with spring constant K, and that the cell pulls through cell-matrix contact. To build up enough force F, the cell has to invest $W = \frac{F^2}{2K}$ into the spring. This implies that the stiffer the string (large K) the less work is needed and the more efficient the build-up of force will be. Equivalently, the cell can invest power L into stretching the spring. The model considers a more realistic scenario where the force activates the cellular response through a certain displacement of elastic components inside the cell. The cell pulls and encounters different elastic environments, each having its own spring constant K. In an isotropic scenario all spring constants are equal. In an anisotropic situation, the cells will prefer various orientations depending on the tensor stress of the environment. The cell prefers to orient itself along the direction of maximal effective stiffness, which can lead to cell locomotion.

Supposing a homogenous external strain, the equation of three-dimensional isotropic elasticity give:

$$\Delta W = -\frac{P_p}{E}[(1+\nu)\cos^2\theta - \nu] \tag{12}$$

θ is the orientation angle relative to the direction of the externally applied tensile stress $p < 0$. Optimal cell orientation corresponds to minimal ΔW, which is achieved when $\theta = 0$, independent of the poission ratio. This means that cells orient preferentially with the direction of stretch. In addition, experimental observations confirm that ΔW decreases with increasing rigidity E.

3.2.2 Notes and Takeaway

This model shows that cell orient themselves to the direction of maximal effective stiffness. This may imply that the stretch in WT and $SMad1/5^{CKO}$ are different. Similarly it could be possible that the orientation of the primary cilia points in the direction of maximal effective stiffness. Similarly this might explain the difference in eccentricity in WT and $SMad1/5^{CKO}$. Another possible hypothesis is that the primary cilia is reoriented in the direction of maximal effective stiffness, and when the primary cilia is streched in the direction of $\phi = 0$ it activates mechanisms in the cell, which allows signals other cells to form columns. This hypothesis assumes the primary cilia acts as both as an input and output sensor for the cell.

3.3 Mathematical Biology Chapter 10: Mathematical modeling of cell-ECM interations [16]

By: J.D. Murray

3.3.1 Overview

The interaction of the cell and the ECM is explored in wound healing. The author provides a mathematical model explaining ECM and cell interactions. The diagram below is our proposal on how chondrocyte cell and viscoelastic extra-cellular matrix are dependent on each other.

$$\Delta \text{ cell density} = \text{passive movement due to ECM deformation} + \text{active movementrelative to ECM} + \text{proliferation/differentiation}$$

$$\Delta\text{ECM density} = \text{movement due to deformation} + \text{synthesis} - \text{degradation}$$

$$\Delta\text{body forces} = \text{traction forces} + \text{ECM resistive forces}$$

The cell coservation equation is:

$$\frac{\partial n}{\partial t} + \nabla \cdot \vec{u}_t = \nabla \cdot (D\nabla n) + rn(n_0 - n) \tag{13}$$

the ECM conservation is given by:

$$\frac{\partial \rho}{\partial t} + \nabla \cdot (\rho \vec{u}_t) = 0 \tag{14}$$

the force equilibrium is given by:

$$\nabla \cdot [\mu_1 \vec{\epsilon}_t + \mu_2 \theta_t \vec{I} + E'(\vec{\epsilon} + \nu' \theta \vec{I}) + \frac{\tau \rho n}{1 + \lambda n^2} \vec{I}] = s\rho\vec{u} \tag{15}$$

Where n is the cell density with n_0 being the steady state value. ρ is the matrix density, $\vec{u}$ is the ECM displacement vector, $\epsilon = .5(\nabla\vec{u} + \nabla\vec{u}^T)$ is the strain tensor, $\theta = \nabla \cdot \vec{u}$ the dilation, $\vec{I}$ the unit tensor, $E' = \frac{E}{1+\nu}$ where E is Young's modulus, nu the Poission ration $\nu' = (\nu/(1-2\nu))$, mu_1, mu_2 are the shear and bulk viscosities, D the cell motility coefficient, r the maximum mitotic rate, s the tethering elasticity coefficient, and λ is a parameter quantifying how cell traction depends on n. The LHS of eq (3) is the active cell traction term, and the RHS is the body force due to subdermal attachments.

4 Evaluation Metrics

4.1 Distance-based columnness (C_{dev})

We ran the columnar interaction model with positional variation for both the wild type (fig 2) and mutant (fig 3). We plotted 5 cells of each column, and automatically generated the line between the centers

of the top and bottom cells, as well as the lines from the centers of each cell horizontal in the x direction to the line connecting the centers of the top and bottom cells. We drew these lines to accentuate the way C_{dev} is computed.

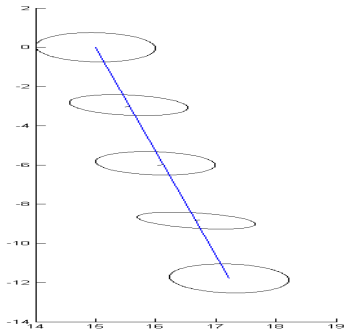

Figure 2: A column generated by the interaction model with positional variation based upon the wild type data. The distances from the center of the cells to the line from the top cell to bottom cell center are denoted with black lines.

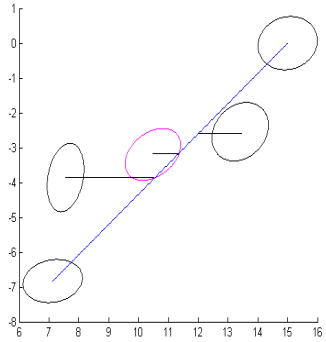

Figure 3: A column generated by the interaction model with positional variation based upon the mutant data. The distances from the center of the cells to the line from the top cell to bottom cell center are denoted with black lines.

4.2 Angle-based columnness (C_{ang})

We then ran the columnar interaction model with positional variation for both the wild type (fig 4) and mutant (fig 5) again, this time emphasizing relevant measures to C_{angle}. Once again, we plotted 5 cells, this time connecting the centers of each cell to the center of the cell and drawing in the angles formed at each vertex in order to accentuate the computation of C_{angle}.

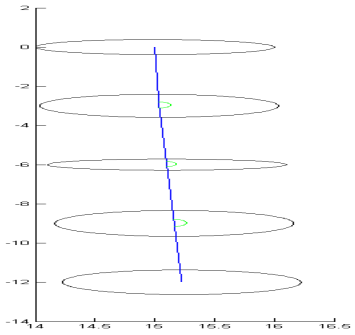

Figure 4: A column generated by the interaction model with positional variation based upon the wild type data. The angles created by the lines connecting cell centers are drawn in green.

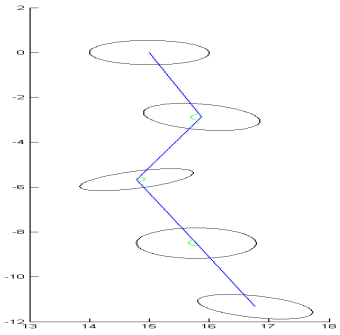

Figure 5: A column generated by the interaction model with positional variation based upon the mutant data. The angles created by the lines connecting cell centers are drawn in green.

5 Results

We performed 1000 simulations of 5 cells of both the wild type and mutant columnar interaction model with positional variation and then performed a two sample unpaired t-test to determine if the C_{dev} is the same for both the wild type and mutant with the null hypothesis that the means are equal. The sample mean of C_{dev} of the wild type was 0.278 with a standard deviation of 0.219, while the sample mean of C_{dev} of the mutant was 0.919 with a standard deviation of 0.733. The difference in the means is 0.641, with a standard error of the difference of 0.024, providing a P value less than 0.0001. We are able to reject the null hypothesis and conclude the C_{dev} for mutant and wild type are different.

We then performed a two sample unpaired t-test to determine if the C_{ang} is the same for both the wild type and mutant with the null hypothesis that the means are equal. We performed 1000 simulations of 5 cells of both the wild type and mutant columnar interaction model with positional variation. The sample mean of C_{ang} of the wild type was 0.106 with a standard deviation of 0.089, while the sample mean of C_{ang} of the mutant was 0.408 with a standard deviation of 0.363. The difference in the means is 0.302, with a standard error of the difference of 0.012, providing a P value less than 0.0001. We are able to reject the null hypothesis and conclude the C_{ang} for mutant and wild type are different.

We also utilized the $\hat{C}$-Function to compare the simulated multi-columnar models to the images and within simulations and images the wild type to the mutant. We observed that the wild type simulation (Fig 6) was able to be differentiated from the mutant simulation (Fig. 8) in terms of $\hat{C}$-Function values, and the $\hat{C}$-Function for wild type (Fig. 7) and mutant (Fig. 9 are easily discernable as well.

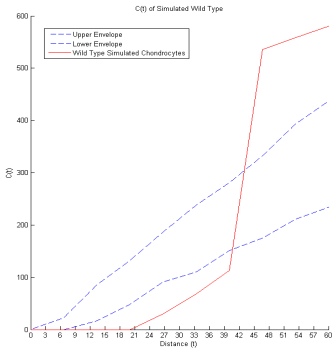

Figure 6: $\hat{C}$-function for the simulated wild type.

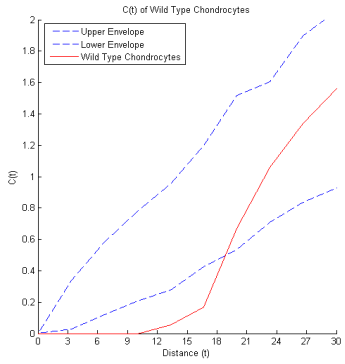

Figure 7: $\hat{C}$-function for the wild type.

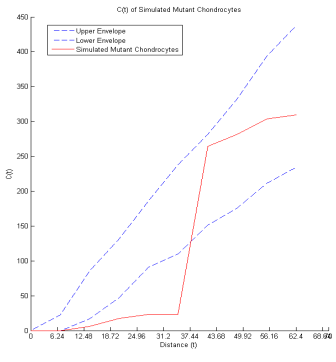

Figure 8: $\hat{C}$-function for the simulated Smad $1/5^{CKO}$ mutant.

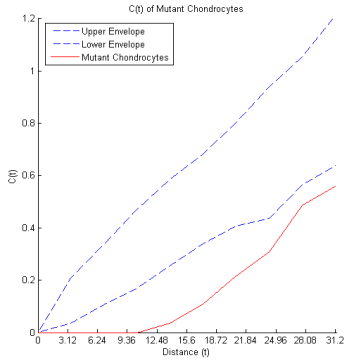

Figure 9: $\hat{C}$-function for the Smad $1/5^{CKO}$ mutant.

References

[1] G Albrecht-Buehler and A Bushnell. The orientation of centrioles in migrating 3t3 cells. *Experimental Cell Research*, 120(1):111–118, Apr 1979.

[2] Attila Aszodi, Ernst B Hunziker, Cord Brakebusch, and Reinhard Fassler. Beta1 integrins regulate chondrocyte rotation, g1 progression, and cytokinesis. *Genes & Development*, 17(19):2465–2479, Oct 2003.

[3] I.B. Bischofs and U.S Schwarz. Cell organization in soft media due to active mechanosensing. *Proceedings of the National Academy of Sciences of the United States of America*, 2003.

[4] Soren T Christensen, Stine F Pedersen, Peter Satir, Iben R Veland, and Linda Schneider. The primary cilium coordinates signaling pathways in cell cycle control and migration during development and tissue repair. *Curr Top Dev Biol*, 85:261–301, 2008.

[5] CE de Andrea, M Wiweger, F Prins, JV Bovee, S Romeo, and PC Hogendoorn. Primary cilia organization reflects polarity in the growth plate and implies loss of polarity and mosaicism in osteochondroma. *Labratory Investigation*, Apr 2010.

[6] G S Dodds. Row formation and other types of arrangement of cartilage cells in endochondral ossification. *The Anatomical Record*, 46(4):385–399, 1930.

[7] Jessica L Feldman, Stefan Geimer, and Wallace F Marshall. The mother centriole plays an instructive role in defining cell geometry. *PLoS Biology*, 5(6):e149, Jun 2007.

[8] R P Gould, L Selwood, A Day, and L Wolpert. The mechanism of cellular orientation during early cartilage formation in the chick limb and regenerating amphibian limb. *Experimental Cell Research*, 83(2):287–296, Feb 1974.

[9] Richard Hall. *A Mathematical Model for Longitudinal Bone Growth*. PhD thesis, Corpus Christi College, University of Oxford, 2000.

[10] Courtney J Haycraft and Rosa Serra. Cilia involvement in patterning and maintenance of the skeleton. *Current Topics in Developmetal Biology*, 85:303–332, 2008.

[11] James L Hayward, Shandelle M Henson, John C Banks, and Sheena L Lyn. Mathematical modeling of appendicular bone growth in glaucous-winged gulls. *Journal of Morphology*, 270(1):70–82, 2009.

[12] E B Hunziker. Mechanism of logitudinal bone growth and its regulation by growth plate chondroctyes. *Microscopy Research and Technique*, 28:505–519, 1994.

[13] S R McGlashan, M M Knight, T T Chowdhury, P Joshi, C G Jensen, S Kennedy, and C A Poole. Mechanical loading modulates chondrocyte primary cilia incidence and length. *Cell Biol Int*, 34(5):441–446, 2010.

[14] D McKenny and J. A. Nickel. Mathematical model for cell division. *Mathematical Computational Modeling*, 25(2):49–52, 1997.

[15] T I Morales. Chondrocyte moves: clever strategies? *Osteoarthritis Cartilage*, 15(8):861–871, Aug 2007.

[16] J.D. Murray. Mathematical biology ii: Spatial models and biomedical applications. pages 491–535, 2004.

[17] S. Ramanti. Mechanical modelling of cell/ecm and cell/cell interactions during the contraction of fibroblast-populated collagen microshpere: theory and model simulation. *Journal of Biomechanics*, 37:1709–1718, 2004.

[18] Kelsey N Retting, Buer Song, Byeong S Yoon, and Karen M Lyons. Bmp canonical smad signaling through smad1 and smad5 is required for endochondral bone formation. *Development*, 136(7):1093–1104, Apr 2009.

[19] Peter Satir, Lotte B Pedersen, and Soren T Christensen. The primary cilium at a glance. *Journal of Cell Science*, 123(Pt 4):499–503, Feb 2010.

[20] Linda Schneider, Michael Cammer, Jonathan Lehman, Sonja K Nielsen, Charles F Guerra, Iben R Veland, Christian Stock, Else K Hoffmann, Bradley K Yoder, Albrecht Schwab, Peter Satir, and Soren T Christensen. Directional cell migration and chemotaxis in wound healing response to pdgf-aa are coordinated by the primary cilium in fibroblasts. *Cellular Physiology Biochemistry*, 25(2-3):279–292, 2010.

[21] Buer Song, Courtney J Haycraft, Hwa-seon Seo, Bradley K Yoder, and Rosa Serra. Development of the post-natal growth plate requires intraflagellar transport proteins. *Developmental Biology*, 305(1):202–216, May 2007.

[22] C H Turner, A G Robling, R L Duncan, and D B Burr. Do bone cells behave like a neuronal network? *Calcified Tissues International*, 70(6):435–442, Jun 2002.

[23] Tony Yeung, Penelope C Georges, Lisa A Flanagan, Beatrice Marg, Miguelina Ortiz, Makoto Funaki, Nastaran Zahir, Wenyu Ming, Valerie Weaver, and Paul A Janmey. Effects of substrate stiffness on cell morphology, cytoskeletal structure, and adhesion. *Cell Motility and Cytoskeleton*, 60:24–34, 2005.

[24] A Zemel, F Rehfeldt, A E F Brown, D E Discher, and S A Safran. Optimal matrix rigidity for stress-fibre polarization in stem cells. *Nature Physics*, 6(6):468–473, 2010.